SEEING

COLIN R. MASSON

Center for Astrophysics, 60 Garden St., Cambridge, MA 02138

Abstract. Atmospheric turbulence limits the resolution of ground-based high-resolution telescopes. In the optical and radio regimes, the seeing may be described in similar ways, although the parameters are different.

1. INTRODUCTION

Atmospheric refractive index variations provide the fundamental limit which restricts the operation of high resolution astronomical instruments, both in the optical and radio regimes. The design of optical interferometers and radio VLBI interferometers is therefore dominated by the seeing constraints. Since there are many good reviews of the observations and physical causes of seeing (e.g. Tatarskii (1971), Wolff (1982), Coulman (1985), Roddier (1981), Baldwin & Wang (1990)), the present review will concentrate on the comparison between optical and radio data, and on recent measurements.

2. DESCRIPTIONS OF SEEING

Seeing is a problem in both optical and radio astronomy, and is caused by the existence of a turbulent atmosphere with fluctuations of path length blowing past the telescope. In both regimes the natural limit to resolution is approximately $1''$, but the optical path fluctuations are dominated by tropospheric density variations, while the radio fluctuations are dominated by humidity variations, since the refractive index of water is ~ 20 times higher at radio than at optical frequencies. At the very lowest radio frequencies, $< 1 GHz$, the resolution is further limited by the ionosphere, which will not be discussed in this paper.

At optical wavelengths ($\lambda \sim 500$ nm), where most telescopes are large filled apertures, long exposures give rise to blurred images, where the angular size of an image, θ, gives an effective telescope diameter, $d_e = \lambda/\theta$, typically ~ 10 cm. Short exposure 'snapshot' images show speckle patterns. A finite time is required for the speckle pattern to change significantly; this 'coherence time' is typically ~ 10 msec.

At radio wavelengths ($\lambda \sim 1$cm), where individual antennas are always small enough to be coherent, atmospheric phase errors were first noticed by interferometers, where it was observed that the rms phase increased with baseline length. However, even at very long baselines, where the signals are incoherent, the instantaneous visibilities and closure phases are still accurate. Even though the peak phase errors may be large, the rates of change are modest, even on the longest baselines, and the 'coherence time' for a significant phase change is typically ~ 1000 sec. A similar effect was noted by Michelson (1920), who observed that the fringes in his stellar interferometer were clearly visible, even in conditions of poor seeing.

A simple description of a wavefront distorted by the atmosphere is shown in the graph in figure 1. A distant source produces plane wavefronts at the top of the atmosphere, which are then wrinkled by the turbulent path fluctuations in the
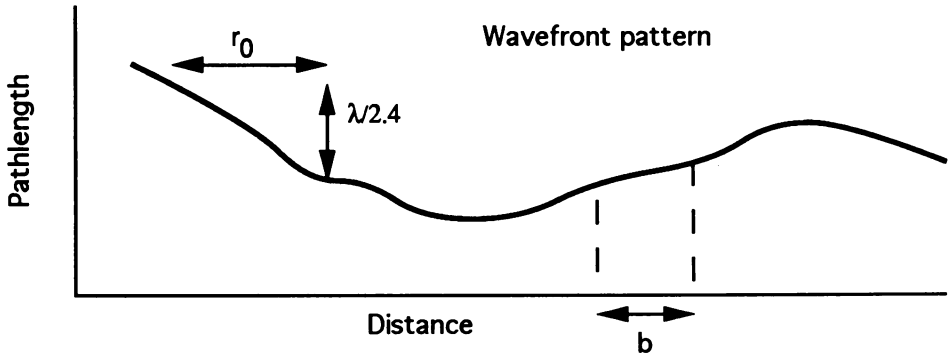
1

Fig. 1. Graph of path error in a wavefront as a function of position. The structure function is the variance of the path difference between two points separated by a distance r. The distance r_0 is defined as the distance where the rms path difference is $\lambda/2.4$

atmosphere. In the Taylor approximation of 'frozen turbulence', the atmosphere blows bodily past the telescope, faster than it can be reorganized by turbulence. As a result, the time variations in the wavefront can be approximated by a simple translation of a single wrinkled pattern. The analysis is simple, since the screen is close to the ground and telescopes are in the near field of most relevant atmospheric fluctuations. The rms pathlength difference between two points on the wavefront increases with their separation, and the coherence distance, r_0, is defined as the separation at which the rms path difference reaches $\lambda/2.4$ (Fried 1965). If the atmosphere moves bodily at a velocity v, there is also a coherence time $t_0 = r_0/v$ in which the path variation above any point is typically $\lambda/2.4$. Note that slightly different definitions of t_0 are used by different authors.

The spatial characteristics of the atmospheric turbulence are most commonly described by the spatial Structure Function, $D(r)$, which is defined as

$$D(r) = \langle (s(x) - s(x+r))^2 \rangle,$$

where $s(x)$ is the path length above a point at position x. The structure function is directly related to the path difference measured by an interferometer with baseline r. Atmospheric turbulence occurs on a wide range of scales and is most conveniently represented by a power law form

$$D(r) = Kr^\beta,$$

although the exponent β typically varies slowly with r. The maximum slope of $\beta = 2$ corresponds to a wedge of path length, giving an angular shift on the sky which is independent of r. Kolmogorov turbulence (e.g. Tatarskii 1961) predicts a slope of $\beta = 5/3$, giving an angular shift which varies as $r^{-1/6}$.

A single power law for the structure function is only an approximation, and a more realistic model includes an inner scale of a few mm where turbulence is damped out, an outer scale where the turbulence is injected, for example by a flow past an obstacle, and an atmosphere with many layers, each with different properties. Some examples of measured radio structure functions are shown by Sramek (1990), illustrating that the structure function of water vapor fluctuations is well represented by a power law over the range of baselines from 0.1 to 20 km.

The temporal characteristics of atmospheric turbulence are related to the spatial characteristics under the hypothesis of frozen turbulence, which implies a one-to-one mapping between time and space. It is then possible to use the structure function to calculate temporal statistics such as the power spectrum of phase variations observed by an interferometer (e.g. Tatarskii 1961, 1971). The graph in figure 1 can be used to understand the effect of fluctuations on different length scales, l, on an interferometer of baseline b. There are two different regimes: i) small spatial scales ($l < b$), which are uncorrelated between the two antennas and which give rise to the faster variations in the power spectrum. These fast variations are independent of b and the variance observed by the interferometer is twice that above a single element. ii) large scales ($l > b$), where the path variations are correlated between the two elements and the variance of the path difference is less than that above a single element. There is a break between these regimes where the spatial wavelength is comparable with the baseline b. At high frequencies (small spatial scales), the power spectrum has the form $P(f) \propto f^{\beta+1}$, and at frequencies below the corner frequency, f_c, the spectrum is $P(f) \propto f^{\beta-1}$. Masson (1993) shows an example of a measured power spectrum for a radio interferometer, while some optical examples are shown by Colavita et al. (1987), and Bester et al. (1992).

Another useful way of describing the temporal statistics is the two-point Allan variance as applied to interferometer phase (Bester et al. 1992), which is essentially the variance in the difference in mean phase between two adjacent time periods, each of length τ. The Allan variance for short times is independent of baseline and has the form $A(\tau) \propto \tau^{\beta}$. There is a turnover at a corner time, $\tau_c \sim b/v$, and at long times the form is $A(\tau) \propto \tau^{\beta-2}$. Bester et al. 1992 show a comparison of three different measures of the temporal variations for a single dataset. The correspondence between the slopes of the several functions is not exactly as expected from the simple calculations above, because the structure function is not a pure power law. The Allan variance is very useful because it is closely related to the coherence time for an interferometer. Since the coherence time depends on the small length scales, it is independent of baseline when b is large.

The discussions above have been based on the assumption that the structure function is a perfect power law at all scales. In general it will not be, and the slopes of the various functions will vary accordingly, although the basic characteristics of coherence lengths and times will not be affected. The most significant such variation expected is an outer scale, beyond which the atmospheric turbulence does not increase, or at least increases very slowly. Such an outer scale could be detected in two different ways. The better method is to measure the spatial structure function and to see a turnover directly, but it is often more practical to use one of the time series methods and to look for features in the power spectrum or Allan variance
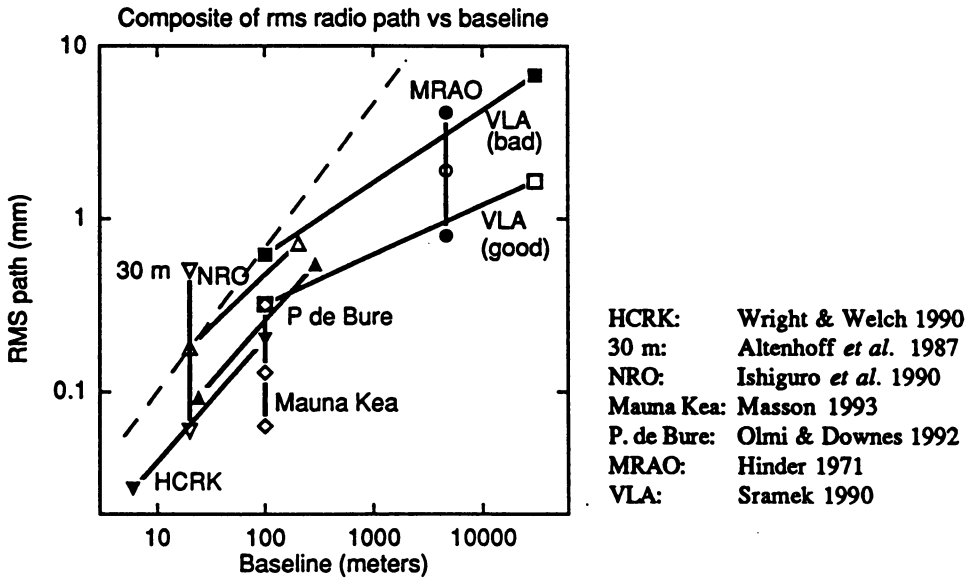
Fig. 2. Composite graph of radio seeing data from many sites. The selection effects and zenith angles are unknown. The dashed line shows the expected slope for Kolmogorov turbulence.

which could not be caused by the finite baseline. However, the latter approach suffers from the limitation that it is based on the assumption of frozen turbulence.

3. MEASUREMENTS OF SEEING

Radio seeing has been measured by many authors, and a composite graph of recent measurements from the literature is presented in figure 2, where the rms path variation (the square root of the structure function) is plotted in units of length as a function of baseline. Most of the measurements were made directly by interferometers, but the so-called 'anomalous refraction' measurements from the IRAM 30m telescope are also included. The measurements cover a wide range of sites and conditions and have unknown selection effects, so they should not be relied upon for comparing sites, although the data from Mauna Kea are based on an unbiased survey covering more than a year and show that it is probably a superior site. The error bars on the point for Mauna Kea show the quartiles of the distribution, illustrating that a wide variety of conditions can be found at any one site.

The remarkable thing is that the data from all the sites are in very good agreement, within a factor of 2 or so. In the region below about 100 m baseline, the graph has a slope of $\beta/2 \simeq 0.7$, or slightly flatter than the Kolmogorov value of 0.83. At longer baselines the slope flattens to $\beta/2 \simeq 0.4$, although there has been no definitive detection of such a turnover in any single dataset. The turnover may be related to the change to 2-dimensional turbulence when the baseline becomes greater than
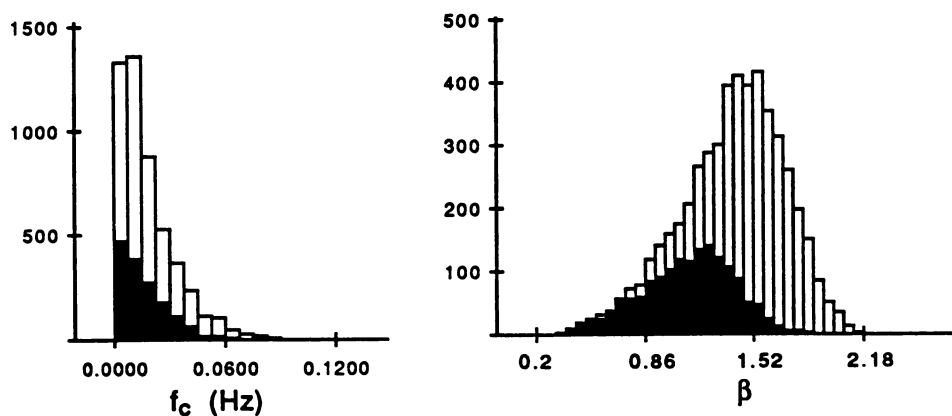
Fig. 3. Distribution of phase power spectrum parameters for data from a 100m radio interferometer on Mauna Kea. The conditions of best seeing have been shaded in both plots.

the effective thickness of the atmosphere (Truehaft & Lanyi 1987). There is a variation of the slope from one time to another (Sramek 1990). The graph in figure 2 shows that the atmosphere has significant turbulence on the largest measured scales of many km.

There are also strong diurnal and seasonal variations, although the details vary from site to site. At Mauna Kea, the rms path error at night is better than the day, and the winter is better than the summer (Masson 1993). There are also correlations between the parameters of the power spectrum, as shown in figure 3. When the corner frequency, which should be proportional to wind speed, is low, the slope tends to be flatter. These conditions are also the times of best seeing.

There are few systematic studies of radio coherence times, although they have been discussed in the context of VLBI (e.g. Rogers and Moran 1981). The coherence time is strongly frequency dependent, but one useful description is to consider a typical windspeed which will relate the spatial and temporal structure functions. For most sites, typical low level winds are $v = 5 \sim 10 m/s$, so the coherence time at any frequency can be estimated from the coherence length r_0 by the relation $t_0 = r_0/v$.

Optical structure functions have been measured by a few authors, and a composite graph of data is presented in figure 4. The measurements have again been adjusted to units of rms path, in microns, as a function of baseline. As in the radio case, there is a remarkable agreement between the different measurements, except for the measurements by Mariotti and Di Benedetto, which were taken on a night of very good seeing. At least for baselines less than 1m, the slope is close to the Kolmogorov value, although there is a real variation of 0.1 or so (Buscher *et al.* 1993). At longer baselines there is an apparently flatter slope, but there is a large scatter, and there are few cases where widely different baselines have been measured
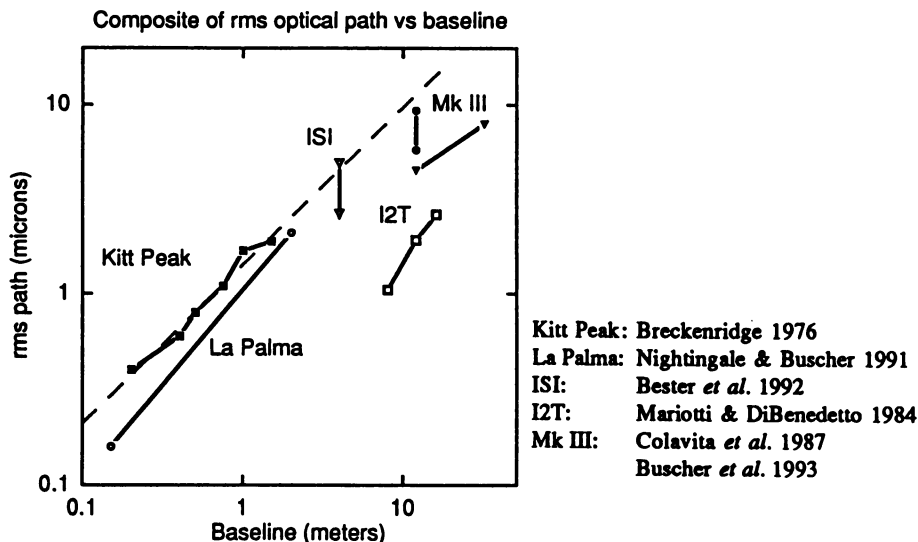
Fig. 4. Composite of optical structure function data. The data have been converted to a common form and are presented as rms path length as a function of distance. The dashed line shows the expected function for Kolmogorov turbulence with $r_0 = 10cm$ at $\lambda = 500nm$.

nearly simultaneously by the same instrument.

Two possible theoretical forms for the outer scale of the structure function are shown in figure 5. The lower curve shows the sharp cutoff of the von Karman spectrum (Tatarskii 1961). Attempts to measure the outer scale of optical turbulence have found no such sharp outer scale, except in occasional cases. The most recent interferometer data (Bester *et al.* 1992; Buscher *et al* 1993) have shown indications of an outer scale in the sense that the slope of the structure function on large baselines is flatter than the Kolmogorov slope. However, even the more gentle form of the Greenwood & Tarrazano (1974) spectrum (see also Truehaft & Lanyi 1987) has too sharp a break to fit observed power spectra (Buscher *et al.* 1993). This is not too surprising if the atmosphere is made up of several layers with different properties, since any outer scale in one layer will be masked by turbulence in another.

As in the radio case, there are indications that the properties of the turbulence are correlated, with better conditions being associated with flatter slopes (Bester *et al.* 1992). Coherence times can be associated with the structure function by an effective windspeed, typically $v \simeq 10m/s$, although there can be significant contributions from upper atmosphere turbulence, where the wind speeds are larger.

In the region of overlap between the optical and radio data, at baseline ~ 10 m, the rms optical path is typically 3 μm, while the radio path variation is typically 50 μm. Considering the scatter in the data and the fact that they are measured at different sites, it is hard to make a firm comparison, but it is interesting that they are
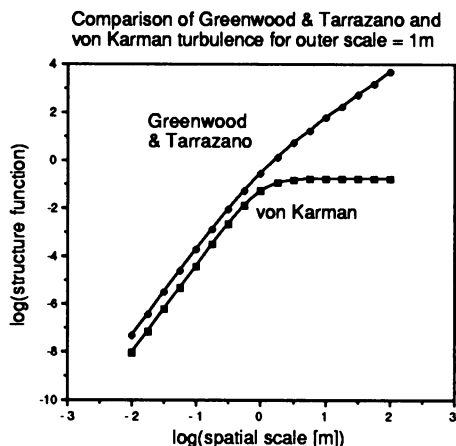
Fig. 5. Predicted Structure functions for two different forms of turbulence.

nearly in the ratio of 20:1, which would correspond to the ratio of refractive indices of water at the two bands. This suggests that a significant part of the optical seeing, at least at long baselines, may be due to water vapor. Furthermore, the increase of the radio structure function to large baselines indicates that there is no sharp outer scale to atmospheric turbulence, although there may be a gentle decrease of slope at large scales. Taking everything together, a reasonable description of the data is that on scales less than 1m, the atmospheric turbulence is well described by Kolmogorov turbulence ($\beta = 1.67$), although a small variation in β is found from one time to another. On scales from 1 - 100 m, there is a gentle decrease to $\beta \simeq 1.4$, while on the largest scales of 0.1 - 10 km, the radio data suggest that $\beta \simeq 1$. The slopes are time variable, with larger variations being found at longer baselines, and flatter slopes being associated with better seeing.

4. APPLICATIONS TO TELESCOPE DESIGN

There are four basic classes of astronomical instruments, when they are divided according to their coherence. This is a wavelength-dependent criterion, so an instrument which is coherent at one wavelength may be incoherent at a shorter one.

1) Coherent filled apertures, such as radio single dishes, or optical interferometer elements. In this case, the diameter, d, is less than the atmospheric coherence length r_0. The aperture is diffraction-limited, with beamsize λ/d, and seeing effects are manifested as pointing fluctuations of angular size $\sqrt{D(d)}/d$, which go as $d^{-1/6}$ in the Kolmogorov case, with a timescale of d/v. For Kolmogorov turbulence, the angular resolution of the largest coherent aperture scales as $\theta \propto \lambda^{-1/5}$.

2) Incoherent filled apertures, such as large optical telescopes, where $d > r_0$. The image breaks up into speckles, each of angular size λ/d, spread over an area of diameter λ/r_0. The speckle pattern changes on the coherence timescale $t_0 = r_0/v$. If adaptive optics are used to correct the aperture, the number of actuators required is $\sim (d/r_0)^2$, and the response time must be faster than t_0.

3) Coherent interferometers, with baseline $b < r_0$, such as small radio interferometers. The beamsize is given by the diffraction limit λ/b, and the phase fluctuations due to the atmosphere have a timescale b/v.

4) Incoherent interferometers, with $b > r_0$, such as optical interferometers, radio VLBI, and the larger configurations of the VLA. Although these interferometers are not coherent in general, a critical point is that the instantaneous fringe amplitudes and closure phases are correct. Provided that there is enough signal/noise to measure these quantities in the coherence time $t_0 = r_0/v$, it is usually possible to reconstruct the absolute phases by various techniques. For optical interferometers, the coherence time is not the only critical parameter, since r_0 determines the size of apertures which can be used, and therefore the signal which can be detected.

Acknowledgements

References

Altenhoff, W. J., Baars, J. W. M., Downes, D.,& Wink, J. E.: 1987, *A&A* **184**, 381

Bester, M., Danchi, W.C., Degiacomi, C.G., Greenhill, L.J. & Townes, C.H.: 1992, *Ap.J.* **392**, 357

Breckinridge, J. B.: 1976, *J.Opt.Soc.Am.* **66**, 143

Baldwin, J. E., & Wang Shouguan: 1990, *IAU Symp. on Radio Astronomical Seeing*, IAP:Beijing

Buscher, D. F., Armstrong, J. T., Mozurkewitch, D., Denison, C. S., Colavita, M. M., & Shao, M.: 1993, in High resolution Imaging by Interferometry, J. M. Beckers & F. Merkle, ed(s)., *Atmospheric Fluctuation Measurements with the MkIII Interferometer*, ESO, *in press*

Colavita, M. M., Shao, M., & Staelin, D. H.: 1987, *Appl.Opt.* **26**, 4106

Coulman, C. E.: 1985, *Ann.Rev.Astr.Ap.* **23**, 19

Fried, D. L.: 1965, *J.Opt.Soc.Am.* **55**, 1427

Greenwood, D. P., & Tarrazano, D. O.: 1974, *RADC Tech. Rep.* **RADG-TR-74-19**,

Hinder, R., & Ryle, M.: 1971, *Mon.Not.R.Astr.Soc.* **154**, 229

Ishiguro, M., Kanazawa, T., & Kasuga, T.: 1990, in IAU Symp on Radio Astronomical Seeing, J. E. Baldwin & Wang Shouguan, ed(s)., *Monitoring of Atmospheric Phase Fluctuations using Geostationary Satellite Signals*, IAP:Beijing, 60

Mariotti, J. M., & Di Benedetto, G. P.: 1984, *I.A.U. Colloq.* **79**, 257

Masson, C. R.: 1993, in IAU Colloq. 140, Astronomy with Millimeter and Submillimeter Wave Interferometry, M. Ishiguro, ed(s)., *Atmospheric Effects and Calibrations*, ASP:San Francisco, *in press*

Michelson, A. A.: 1920, *Ap.J.* **51**, 257

Nightingale, N. S., & Buscher, D. F.: 1991, *Mon.Not.R.Astr.Soc.* **251**, 155

Olmi, L., & Downes, D.: 1992, *Astr.Ap.* **262**, 634

Roddier, F.: 1981, *Prog.Opt* **19**, 281

Rogers, A. E. E., & Moran, J. M.: 1981, *I.E.E.E.Trans.Inst.Meas.* **IM-30**, 283

Sramek, R. A.: 1990, in IAU Symp on Radio Astronomical Seeing, J. E. Baldwin & Wang Shouguan, ed(s)., *Atmospheric Phase Stability at the VLA*, IAP:Beijing, 21

Tatarskii, V. I.: 1961, *Wave Propagation in a Turbulent Medium*, Dover:New York

Tatarskii, V. I.: 1971, *The Effects of the Turbulent Atmosphere on Wave Propagation*, Israel Program for Scientific Translations:Jerusalem

Truehaft, R. N., & Lanyi, G. E.: 1987, *Radio Sci.* **22**, 251

Woolf, N. J.: 1982, *Ann.Rev.Astr.Ap.* **20**, 367

Wright, M. C. H. & Welch, W. J.: 1990, in IAU Symp on Radio Astronomical Seeing, J. E. Baldwin & Wang Shouguan, ed(s)., *Interferometer Measurements of Atmospheric Phase Noise at 3 mm*, IAP:Beijing, 71

Discussion:

Simon:
The work by Buscher, and also by Colavita, with the Mark III interferometer suggests that the atmosphere is usually closely approximated by a Kolmogorov spectrum with an outer scale **much greater** than the longest baseline of $\sim$ 30 meters. A small fraction of the time we see large deviations from a Kolmolgorov spectrum, with strong evidence for an outer scale of $\sim$ 100 m.

Masson:
The recent preprint by Buscher et al. shows that there is evidence for flattening of the spectrum on scales $\sim$ 10 m, although the temporal power spectra showed that the outer scale was not sharp.

Gonglewski:
You list the structure function "keel-over" as a method for searching for the outer scale. This is an extremely dangerous method since it works only for **true** short exposures, i.e. all non-short exposures exhibit a false outer scale. (See Heidbreider.)

Masson:
Measurement of the structure function is the only method which avoids the assumption of frozen turbulence. Care must be taken to avoid artifacts with any method, but most modern radio and optical interferometers have sufficiently fast sampling to measure the relevant fluctuations. A bigger limitation for current optical interferometers is that only a small number of baselines is present simultaneously.